Mathematical Modeling of the Cloudiness Effect on Atmospheric Gas Composition

V.O. Arutyunyan[1], A.E. Aloyan[1], A.N. Yermakov[2]
[1]Institute of Numerical Mathematics, Russian Academy of Sciences,
Gubkin str., 8, 119333, Moscow, Russia
[2]Institute of Energy Problems of Chemical Physics, Russian Academy of Sciences,
Leninski pr. 38/2, 119334, Moscow, Russia

1. Introduction

Clouds constitute a key climate-forming mechanism influencing on the longwave (heat) and shortwave (solar) radiation balance. The indirect climate impact of clouds is caused by variations in the gas species and aerosols in the atmosphere. The main components of this impact are: (1) the change in concentrations of trace gases and aerosols due to convective transport from lower to upper layers of the atmosphere, (2) wet removal of gas species and aerosols from the boundary layer, and (3) heterogeneous chemical reactions with participation of ice particles and cloud drops. The importance of these processes for the chemical composition of the atmosphere is testified by data of model experiments; however, there have been uncertainties in understanding their mechanisms and behavior in the atmosphere. Among gas species, most sensitive to cloud formation are sulfur-containing admixtures, which finally are converted into well-soluble sulfates serving as effective condensation nuclei. The sulfur-containing admixtures are oxidized not only in the gas phase but also in the cloud phase. Because of this, the lifetimes of some admixtures chemically converting into aerosol particles are considerably higher in the free atmosphere than in the boundary layer. Falling into upper layers of the atmosphere, these admixtures can travel to long distances.

In this work, we consider a 3D numerical model of convective cloudiness with detailed microphysics and gas/aqueous-phase chemistry. The model does not include the microphysical processes leading to ice formation since our main aim here was to assess the size effects in the formation of ion composition of the cloud drop phase. The description of basic models can be found in (Aloyan, 2008; Aloyan et al., 2010). It should be noted that in models like ours the aqueous-phase reactions (including those with the participation of transition metals) usually have not been given due consideration. The model used by us (Reduced Model, RM) (Yermakov et al., 2003) for describing the SO_2 oxidation in a convective cloud is a compromise between the degree of detail and the number of chemical reactions.

2. Model Description

2.1 Dynamical Framework

The equations of motion for moist convection are represented as

$$\frac{\partial}{\partial t}\left(\bar{\rho} u_i\right)+\frac{\partial}{\partial x_j}\left(\bar{\rho} u_j u_i\right)=-\frac{\partial p'}{\partial x_i}-2\varepsilon_{ijk}\bar{\rho}\Omega_j u_k+\delta_{i3}\bar{\rho} g\left(\frac{\vartheta'}{\bar{\vartheta}}+\varepsilon q'_v-Q_w-\frac{p'}{k\bar{P}}\right)+\frac{\partial T_{ij}}{\partial x_j} \ . \tag{1}$$

Here ε_{ijk} is the absolute symmetric tensor, δ_{ij} is the Kronecker delta, Ω_i is the vector of the Earth's angular velocity, g is the gravitational settling, $k = c_p/c_v$ is the adiabatic index, $\varepsilon = 0.608 = R_d/R_v$, where R_d and R_v are the specific gas constants for dry air and water vapor, respectively, Q_w is the mixing ratio of liquid water, and τ_{ij} is the Reynolds stress.

The equation of continuity has the form

$$\frac{\partial \bar{\rho} u_j}{\partial x_j}=0 \ . \tag{2}$$

The equations for potential temperature and specific humidity are written as

$$\frac{\partial}{\partial t}\left(\bar{\rho}\vartheta\right)+\frac{\partial}{\partial x_j}\left(\bar{\rho} u_j \vartheta\right)=\frac{L_c \vartheta}{c_p \bar{T}}\frac{dM_c}{dt}+\frac{\partial}{\partial x_j}\left(\bar{\rho} K_H \frac{\partial \vartheta}{\partial x_j}\right), \tag{3}$$

$$\frac{\partial}{\partial t}\left(\bar{\rho} q_v\right)+\frac{\partial}{\partial x_j}\left(\bar{\rho} u_j q_v\right)=\frac{dM_c}{dt}+\frac{\partial}{\partial x_j}\left(\bar{\rho} K_H \frac{\partial q_v}{\partial x_j}\right), \tag{4}$$

where ϑ is the potential temperature, q_v is the specific humidity, L_c latent heat of condensation, d Mc/dt describes the water vapour mass condensing (evaporating) per time unit, K_H is the coefficient of turbulent diffusion, T is the absolute temperature, p is pressure, and ρ is the air density.

2.2 Microphysics

The microphysics in the cloud system is described with the help of two distribution functions $n_1(x_i, r_n, t)$ for cloud condensation nuclei (CCN) and $n_2(x_i, m, t)$ for cloud drops (Kogan, 1991).

The equation for CCN is written as

$$\frac{\partial n_1}{\partial t}+\frac{\partial}{\partial x_j}\left(u_j n_1\right)=-\left[\frac{\partial n_1}{\partial t}\right]_{\text{nucl}}+\frac{\partial}{\partial x_j}\left(K_H \frac{\partial n_1}{\partial x_j}\right), \tag{5}$$

The equation for the distribution function of drops takes into account advective and turbulent transport as well as changes due to sedimentation, condensation/evaporation, and coagulation:

$$\frac{\partial n_2}{\partial t} + \frac{\partial}{\partial x_j}\left(\left(u_j - w_g(m)\delta_{i3}\right)n_2\right)$$
$$= \left[\frac{\partial n_2}{\partial t}\right]_{\mathrm{nucl}} + \left[\frac{\partial n_2}{\partial t}\right]_{\mathrm{cond}} + \left[\frac{\partial n_2}{\partial t}\right]_{\mathrm{coag}} + \frac{\partial}{\partial x_j}\left(K_H \frac{\partial n_2}{\partial x_j}\right), \tag{6}$$

where $w_g(m)$ is the rate of fall of drop with mass m.

2.3 Nucleation, Condensation/Evaporation, and Coagulation

The value of air humidity at which the cloud drop is in equilibrium with ambient vapor differs from the saturating humidity over a flat surface. This is caused, firstly, by curvature of the drop surface and the related surface tension and, secondly, by drop salinity. The contributions of these effects are opposite in sign, and the equilibrium for the given drop is determined by Kohler's formula (Pruppacher and Klett, 1978). When CCN are activated, their further growth is described by the equation of drop growth (Mordy, 1959). The change of cloud drop size distribution due to coagulation is described by the Smoluchowsky equation. The coagulation coefficient is considered for all collision regimes: diffusion, free-molecular, and gravitational.

2.4 Chemical Processes in Convective Clouds

The gas- and aqueous-phase transport of pollutants for the one-dimensional case is described by the following system of nonlinear differential equations (Yermakov et al., 2003; Hermann et al., 2000):

$$\frac{d[C_g^i]}{dt} = w^i_{gen,g} - w^i_{loss,g} - \left([C_g^i]k_i - [C_{aq}^i]\frac{k_i}{K_H^i k_b T}\right)L, \tag{7}$$

$$\frac{d[C_{aq}^j]}{dt} = wj^j_{gen,aq} - w^j_{loss,aq} + \left([C_g^i]k_i - [C_{aq}^j]\frac{k_i}{K_H^i k_b T}\right)\frac{1}{N_A}, \tag{8}$$

where C_g^i and C_{aq}^j are the concentrations of the i-th gas-phase component (cm^{-3}) and j-th aqueous-phase component (mole/l), $i = 1, \ldots, N_g$; $j = 1, \ldots, N_{aq}$; N_g and N_{aq} are the numbers of species in gas and aqueous phases, respectively, $w^i_{gen,g}$ and $w^i_{loss,g}$ are the generation and loss rates of the i-th component in gas-phase reactions ($cm^{-3}s^{-1}$), $w^j_{gen,aq}$ and $w^j_{loss,aq}$ are the generation and loss rates of the j-th component in aqueous-phase reactions (mole/(l·atm)), k_b is the Boltzmann constant, and N_A is the Avogadro number. The transition between gas and aqueous phases is described by the resistance model (Schwartz, 1988). Equations (5) and (6) describe the balance of flows of a given species in the gas and aqueous phases, respectively. The model incorporates 51 aqueous-phase and 31 gas-phase species. This system of ODEs is solved using a numerical algorithm described in (Aloyan et al., 2010).

3. Results of Numerical Experiments

Numerical experiments were performed to simulate the moist convection and cloud formation in the atmosphere. The horizontal size of the modeling domain 20 x 20 km with a 500 m step size, the height of the domain is 2.5 km with 50 100-m vertical layers (except the first layer, which is 50 m), the time step is 150 s, the CCN concentration was taken to be 380 cm^{-3} at the level of 500 m and exponentially decreasing above 500 m. The main source of convection was an initially given temperature perturbation with its value specified for the Earth's surface and decreasing with height.

3.1 Formation of Convective Cloudiness

The calculations were performed for clouds of small vertical power, which is conditioned by the fact that our model is designed for drops and the tops of more powerful clouds can rise significantly higher than the level of the zero isotherm. At the initial stage of cloud formation, the nucleation and condensation processes are dominant and the drop-size distributions are unimodal at all points. The further cloud processing is characterized by an ever growing impact of coagulation and sedimentation (along with condensation) on the distributions. As a result, the drop-size distribution becomes bimodal for the whole cloud, and the fraction of small drops in the water content decreases. Figure 1 shows the number concentrations of cloud drops of different sizes at 1200 m after 3 hours of simulations. It can be seen a concentration decrease at the cloud center. The presence of negative temperature perturbations in clouds is not uncommon, in this case, the maximum of water content reaches 2–3 g/kg, which is consistent with experimental data.

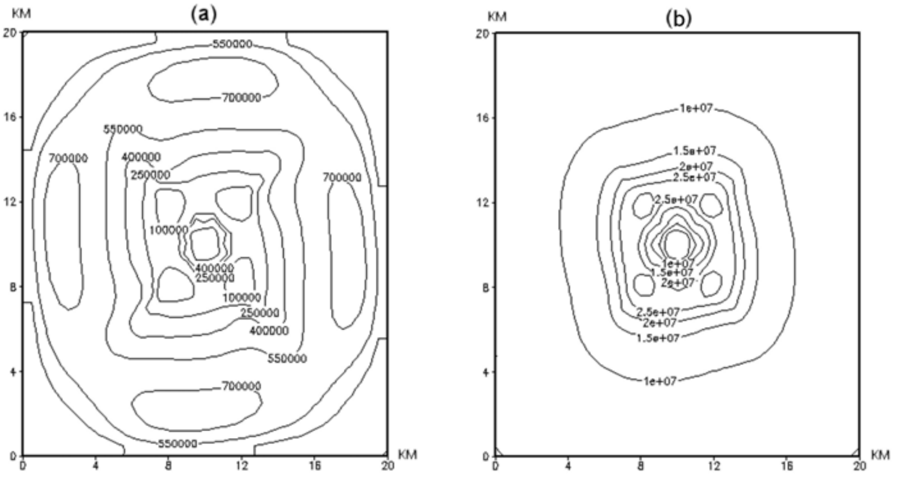

Number concentrations of cloud drops of sizes (a) 10 μm and (b) 50 μm at 1200 m after 3 hours of simulations.

3.2 Chemical Transformations in the Atmosphere

In cloud drops, $SO_{2(g)}$, $NO_{2(g)}$, and other species absorbed from air are subjected to oxidation. In daytime, this process is caused by the $O_{3(g)}$ and $H_2O_{2(g)}$ gas intake. In the nighttime, the decisive role is played by the $NO_{3(g)}$ gas intake as well as the generation of $SO_{3(aq)}^-$ radicals in the reaction $FeOH_{aq}^{2+} + HSO_{3(aq)}^- \rightarrow SO_{3(aq)}^-$. In the reduced model used by us, the oxidation of $SO_{2(g)}$, $NO_{2(g)}$, and other species is based only on the most significant processes (Yermakov et al., 2003). The numerical calculations indicated that, in areas close to the emission source, $[OH_g]$ rather quickly (in around 1000 s) reaches its quasistationary level ($\approx 5 \cdot 10^4$ cm^{-3}). This value of $[OH_g]$ is controlled by the reaction $OH_g + SO_{2(g)}$, which inhibits the process OH + CO and leads to a sharp decrease in $[HO_{2(g)}]$. The cloud formation merely slightly reduces the value of $[OH_g]$ (by around 30%). This is caused by the dissolution of OH and relevant chemical reactions in the drop phase. In this case, the concentration turns out to be higher in smaller size drops. The cloud formation has an essentially greater impact on $[HO_{2(g)}]$. Its concentration in larger drops is an order of magnitude lower than in smaller size drops. The cloud formation affects dramatically the content of $[HO_{2(g)}]$ in gas. In the course of this process, $[H_2O_{2(g)}]$ is reduced in several orders of magnitudes from approximately $2 \cdot 10^{10}$ to 10^6 cm^{-3}. This considerable effect is caused by the sharp fall of $[HO_{2(g)}]$ and high solubility of hydrogen peroxid. Here, the most part of $H_2O_{2(g)}$ dissolves in small drops (10÷30 μm), because the drop moisture is mainly concentrated there (> 90%). The drops of these sizes are characterized by major dissolution of sulfuric dioxide, which leads to rather increased initial acidity of drops (pH 4.5) assisting in the autocatalytic reaction $H_2O_{2(aq)} + HSO_{3(aq)}^- + H_{aq}^+ \rightarrow SO_{4(aq)}^{2-} + 2H_{aq}^+ + H_2O_l$. This process is terminated when $H_2O_{2(g)}$ is exhausted in the gas. No competition can be found by the reactions $O_{3(aq)}$ + $SO_{2(aq)}/HSO_{3(aq)}^-$, because the solubility of ozone is very low. The numerical calculations indicated that in the course of cloud processing the content of sulfate ions in small drops is reduced, while, in large drops, it grows. This testifies that the sulfuric and other acids in small drops go in part to larger drops.

Within the frameworks of the GDF experiment (Choularton et al., 1997), we revealed some reduction of $[SO_{2(g)}]$ due to a contact of the polluted air with cloud. The averaged rate of $[SO_{2(g)}]$ reduction was ≤ 1 ppb/h for the cloud formation episode of May 5, 1993 (19:00–21:00). The volume content liquid water in air (L) during the air motion varied in the range from $(3.5 \pm 0.13) \cdot 10^{-7}$ to $(1 \pm 0.05) \cdot 10^{-7}$, and $[SO_2(g)]$ varied between 0.43 ± 0.43 and 0.37 ± 0.18 ppb. In the episodes of cloud formation on May 9 and 10, 1993, the time-averaged rate of decrease of $[SO_2(g)]$ was equal to 5 and 4 ppb/h, respectively. These values are not too different from the rate calculated by us in this study: ≈ 102 ppb/h for $[SO_2\ (g)] \approx 60$ ppb, $[H_2O_2\ (g)] = 0.9$ ppb, and $L \approx 2 \cdot 10^{-5}$. The results of our calculations for the distribution of iron ions in atmospheric drops are not too different from field observation data available in the literature; for example, for the so-called radiation fog drops (Behra and Sigg, 1990) in nighttime, the observed value is $[Fe(II)]/[Fe]_{tot} \approx 0.2$, where $[Fe]_{tot}$ is the total content of iron ions in clod drops.

This study was supported by the Russian Foundation for Basic Research, project nos. 09-05-00270 and 09-05-00281.

References

Aloyan A.E., Modeling the Dynamics and Kinetics of Gas Admixtures and Aerosols in the Atmospheres, 2008, Moscow, Nauka (in Russian).

Aloyan A.E. and Piskunov V.N., Modeling the regional dynamics of gaseous species and aerosols in the atmosphere, 2005, Izvestiya RAN: Atm. Ocean. Physics, 41(4), 328-340.

Aloyan A.E., Yermakov A.N., Arutyunyan V.O., and Zagaynov V.A., 2010, Dynamics of gaseous species and aerosols in the atmosphere with heterogeneous processes on the surface of particles, Izvestiya RAN: Atm. Ocean. Physics, 44(3), 120-134.

Behra P., Sigg L., Evidence for redox cycling of iron in atmospheric water droplets, 1990, Nature, 344, 419-421.

Choularton T.W., Colville R.N., Bower K.N. et al., 1997, The Great Dun Fell Cloud Experiment 1993: an overview, Atmospheric Environment, 31(16), 2393-2405.

Herrmann H., ErveHerrns B., Jacobi H.-W., Wolke R., Nowacki P., and Zellner R., 2000, CAPRAM2.3: A chemical aqueous-phase radical mechanism for tropospheric chemistry, J. Atmos. Chem., 2000, 36(3), 231-284.

Kogan Y.L., 1991, The simulation of a convective cloud in a 3-D model with explicit microphysics. Part I: Model description and sensitivity experiments, J. Atmos. Sci., 48, 1160-1189.

Mordy W., 1959, Computations of the growth by condensation of a populations cloud drops, Tellus, 11, 11-64.

Pruppacher H.R. and Klett J.D., 1978, Microphysics of clouds and precipitation. Dordrecht: Reidel.

Schwartz S.E., 1988, Mass-transport limitation of the rate of in-cloud oxidation of SO_2: re-examination in the light of new data, Atmospheric Environment, 22, 2491-2499.

Yermakov A.N., Larin I.K., Ugarova A.A., and Purmal A.P., 2003, Catalysis of SO_2 oxidation by iron ions in the atmosphere, Kinetics and Catalysis, 44(4), 524-537.